RSC Advances

RSCPublishing

PAPER

View Article Online
View Journal | View Issue

Cite this: *RSC Advances*, 2013, **3**, 1922

Photodecomposition of *N*-hydroxyurea in argon matrices. FTIR and theoretical studies†

Magdalena Sałdyka

Received 30th October 2012, Accepted 21st November 2012

DOI: 10.1039/c2ra22694d

www.rsc.org/advances

The photochemistry of *N*-hydroxyurea in solid argon has been investigated by FTIR and *ab initio* calculations. The irradiation of the $NH_2CONHOH$/Ar matrices with the full output of the Xe arc lamp leads to the formation of the HNCO–NH_2OH and N_2–H_2O–CO complexes. For the isocyanic acid–hydroxylamine complex, the spectra prove the existence of the hydrogen bonded structure with the NH group of HNCO attached to the oxygen atom of the NH_2OH molecule. Two structures were identified for the nitrogen–water–carbon monoxide complex. In the first one, water is hydrogen bonded to the carbon atom and interacts with the nitrogen atom through van der Waals forces. In the second structure, water serves as a proton donor toward the nitrogen and carbon atoms of N_2 and CO molecules, respectively. The identification of the products is confirmed by deuterium substitution and by MP2 calculations of the structure and vibrational spectra of the identified complexes.

1. Introduction

N-hydroxyurea (HU) was first synthesized in the 1860s.[1] After it was found to be active against a variety of tumors, HU was shown to inhibit DNA synthesis[2] by inhibiting ribonucleotide reductase.[3,4] As a result, HU has become standard therapy for chronic myelogenous leukemia, polycythemia vera, and myeloproliferative disorders.[5] HU is considered an effective systemic agent for the control of severe psoriasis[6] and a complement to radiation treatment in patients with carcinoma of the cervix and in head and neck cancer.[7] Recently, it was reported that HU could stimulate fetal hemoglobin synthesis and had been successfully used to treat sickle cell anemia.[8] HU is also an immunomodulatory agent that has been documented to enhance the antiretroviral activity of nucleoside reverse transcriptase inhibitors in HIV.[9,10] HU acts as a source of nitric oxide, which plays an important role in the maintenance of normal blood pressure and flow.[11] Growing evidence indicates the *in vivo* conversion of HU to nitric oxide in sickle cell disease patients undergoing *N*-hydroxyurea therapy.[12] Both chemiluminescence detection experiments and EPR spectroscopy show the formation of NO and NO-related species from *N*-hydroxyurea in humans.[13]

Since *N*-hydroxyurea is a representative of hydroxamic acids (RCONHOH), presentation of some issues concerning photochemistry of this class of compounds seems essential for this study. As can be found in literature, photoirradiation of hydroxamic acids may lead to an initial photolytic scission of the N–O bond. In 1960 Walling and Naglieri[14] reported the photolytic scission of the N–O bond in *N*,*O*-diacylbenzoylhydroxylamine. The formation of anilides and amides after photoirradiation of *N*-substituted naphthalenehydroxamic acids[15] and *N*-phenylbenzenehydroxamic acids,[16,17] as well as 2-(arylthio)-benzenehydroxamic acids[18,19] and 2-(aryloxy)benzenehydroxamic acids,[20] is also consistent with the initial homolysis of the N–O bond. Benzyl *N*-methylbenzohydroxamate was suggested to undergo photoelimination in the singlet state through a mechanism involving N–O bond cleavage.[21] In addition to the photolytic N–O bond scission, other mechanisms of the photolysis of hydroxamic acids have also been reported. The photoirradiation of selected naphthalenehydroxamic acids[22] suggests that photoirradiation of these compounds leads to acylaminoxyl radical generation and not to the scission of the N–O bond. It has been suggested that acylaminoxyl radicals are primary intermediates in the photochemical reaction of *N*-substituted hydroxamic acids containing the hydroxyl groups.[15,17]

I have recently reported the isomerical and structural properties of *N*-hydroxyurea.[23] The importance of this molecule for medical and pharmaceutical applications triggers questions about the influence of UV-Vis irradiation on the structure and photochemical properties of HU, especially in view of the results of the recent biological studies showing the *N*-hydroxyurea molecule as an important nitric oxide donor.[11] In the recent paper of our research group,[24] we showed that the UV-Vis photodecomposition of the simplest representative of hydroxamic acids, namely formohydroxamic acid (HCONHOH), in low temperature matrices leads to the HNCO + H_2O and NH_2OH + CO products, which suggests two photodissociation channels proceeding through the

---

Faculty of Chemistry, University of Wrocław, F. Joliot-Curie 14, 50-383 Wrocław, Poland. E-mail: magdalena.saldyka@chem.uni.wroc.pl

† Electronic Supplementary Information (ESI) available. See DOI: 10.1039/c2ra22694d

scission of the N–O or C–N bonds. If the HU molecule exhibits similar mechanisms of photodissociation to the formohydroxamic acid molecule, then the photodissociation of HU should produce the HNCO–NH_2OH and NH_2NHOH–CO complexes as photoproducts. In this paper, for the first time, the photochemical behaviour of *N*-hydroxyurea in an argon matrix is presented.

2. Experimental

Infrared matrix isolation study

The studies were performed for $NH_2CONHOH$/Ar and $ND_2CONDOD$/Ar samples. The solid sample of HU was placed in a small electric oven assembled inside the cryostat. The temperature of the oven was controlled by a DC regulated power supply (NDN instruments). Matrices were prepared by co-deposition of HU vapour coming out of the oven with a large excess of argon onto the cold CsI window. The low temperature was maintained by means of a closed cycle helium refrigerator (ARS-2HW). FTIR spectra were recorded between 4000–500 cm^{-1} in transmission mode by means of a Bruker 66 FTIR spectrometer with a resolution of 0.5 cm^{-1} and using a liquid N_2 cooled MCT detector.

After the infrared spectra of the initially deposited matrices were recorded, the samples were exposed to the full output irradiation of a Xe arc lamp (Osram, XBO 450 W) for up to 300 min. A 5 cm water filter served to reduce the amount of infrared radiation reaching the matrix.

A few experiments were performed for H_2O/CO/Ar samples prepared by the standard manometric technique; the concentration of the gas mixture varied in the range from 1 : 1 : 1000 to 1 : 1 : 2000.

Computational details

All calculations were performed using the Gaussian09 code.[25] Since most of the considered complexes are weakly bonded, the structures were optimized in two steps at the MP2 computational level with the 6-311++G(2d,2p) and aug-cc-pVTZ basis sets. First, standard geometry optimization of each complex was carried out. Afterwards, all the structures found were reoptimized with the counterpoise correction (CP).[26,27] Both normal and CP-corrected harmonic wavenumbers and intensities were obtained for the optimized complexes. The anharmonic wavenumbers for the species identified in the performed experiments were also calculated on the MP2/aug-cc-pVTZ level. A potential energy distribution (PED) of the normal modes was computed in terms of symmetry coordinates with the GAR2PED program.[28]

3. Results and discussion

Photolysis of HU/Ar and HU-d_4/Ar matrices

Fig. 1–3(a–c) show the selected spectral regions of $NH_2CONHOH$ isolated in solid argon, recorded directly after matrix deposition (a), after matrix irradiation with the Xe arc lamp for 180 min (b) and after annealing of matrix b for 10 min to 30 K (c). Fig. 2(d) and Fig. 4 present the spectra of the $ND_2CONDOD$/Ar matrix after 180 min irradiation.

The spectra of *N*-hydroxyurea and its deuterated isotopomer in solid argon have been previously reported.[23] As discussed in that paper, in the spectra recorded directly after matrix deposition, strong bands due to 1*Ea*-HU and weak bands due to 1*Za*-HU isomers were identified. Matrix irradiation leads to a simultaneous decrease of the bands due to the HU isomers and appearance of new product bands. All new bands that appear in the spectra of photolysed matrices are assigned to HU photodissociation products and are collected in Table 1. New vibrational features are observed in the typical regions of water absorptions (3700–3600 cm^{-1} and 1650–1580 cm^{-1}), isocyanic acid (HNCO) (2280–2200 cm^{-1}), carbon monoxide (CO) (2160–2130 cm^{-1}) and hydroxylamine (NH_2OH) (3630–3600 cm^{-1} and 1150–1100 cm^{-1}). The performed experiments allowed us to distinguish three main groups of bands, labelled as 1, 2a and 2b, which respond in different ways to the photolysis of HU/Ar matrices and to annealing processes. Matrix annealing leads to an increase of the bands of group 2a and a disappearance of the bands due to group 2b, whereas the bands assigned to group 1 decreased in intensity. The absorptions attributed to group 1 appear at 3631.8, 3630.6, 3287.9, 3285.2, *ca.* 2264.0, 1613.4, 1148.3 and 898.0 cm^{-1} in the spectra of irradiated HU/Ar matrices. The bands due to groups 2a and 2b are observed at 3728.4, 3722.0, 3638.0, 3624.8, 2148.9, 2148.5, 1598.7, 1595.0 cm^{-1}. As will be discussed below, the bands due to group 1 can be assigned with confidence to the HNCO–NH_2OH complex and the bands of group 2a and 2b to the N_2–H_2O–CO complexes.

In addition to the above mentioned band sets some medium and weak intensity absorptions also appeared in the HU/Ar matrix spectra after photolysis (see Table 1 and Fig. 1–4); their assignment can be made on the basis of the literature data. The bands at 3295.2, 574.5 and 2146.3, 1600.8, 1121.6 cm^{-1} are due to the HNCO–H_2O and NH_2OH–CO complexes, respectively.[24] The absorption appearing at 2138.4 cm^{-1} is due to the CO monomer[29] and the weak band at 2142.6 cm^{-1} is attributed to the CO complex with NH radical.[30] The very weak absorptions at 2885.3, 2816.5, 1610.2, 1499.0 and 1173.8 cm^{-1} are assigned to the H_2CO–H_2O complex and the 2796.0 cm^{-1} band is due to the H_2CO monomer, in agreement with the literature data.[31] In the HU-d_4/Ar matrix spectra after photolysis the very weak bands at 2693.4, 2689.5, 2688.2 and 1171.8 cm^{-1} are attributed to the hydroxylamine-d_3 monomer.[32] Three very weak absorptions at 2635.0, 2284.5 and 1077.6 cm^{-1} are assigned to the DOCN molecule.[33] The 2747.5, 2623.2, 2084.7, 1690.9, 1190.0 cm^{-1} bands are due to the D_2CO–D_2O complex and the 2071.3 cm^{-1} band is assigned to the D_2CO monomer.[31]

Formation of the HNCO–NH_2OH complex

The bands due to set 1 appeared in regions of the most intense absorptions of isocyanic acid vibrations and in the vicinity of the hydroxylamine monomer bands.

The IR spectra of HNCO in low temperature matrices have been reported.[33] The HNCO monomer isolated in an argon matrix is characterized by a very strong band of the NCO antisymmetric stretching vibration at 2259.0 cm^{-1} and weaker

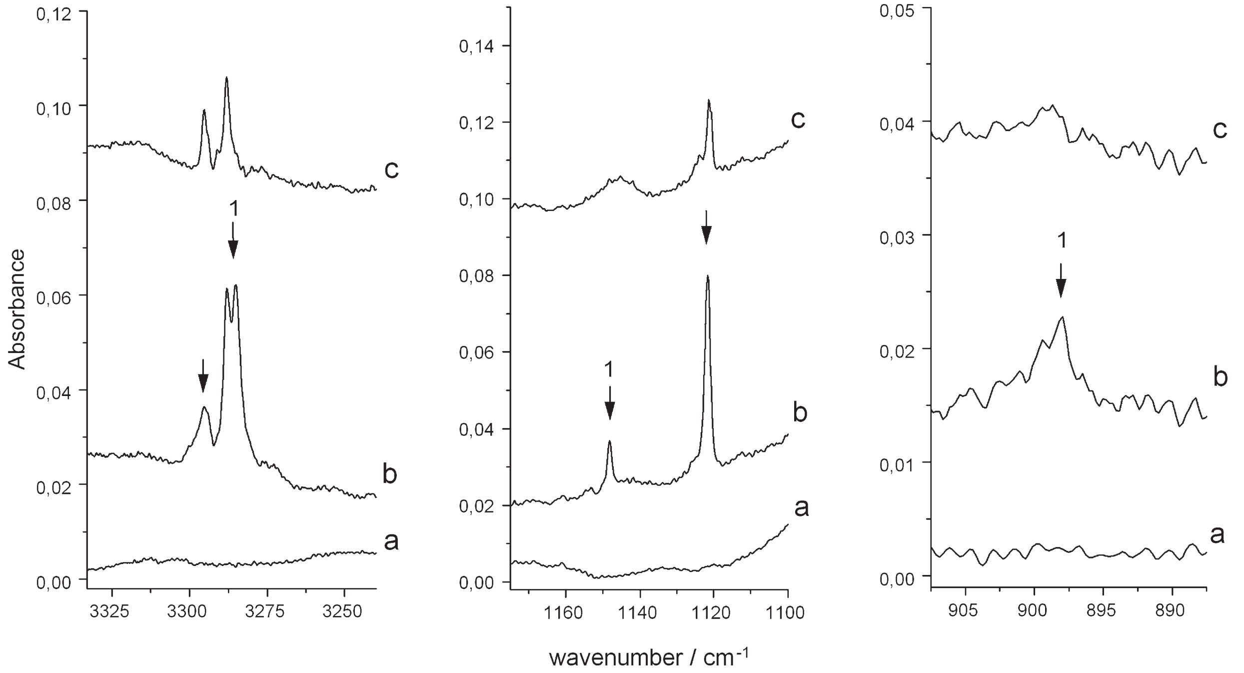

Fig. 1 The selected regions in the spectra of matrices: $NH_2CONHOH/Ar$ after matrix deposition at 15 K, spectrum measured at 9.5 K (a), after matrix irradiation with the full output of Xe arc lamp for 180 min (b), and after annealing of matrix b for 10 min in 30 K, spectrum measured at 9.5 K (c).

bands due to the NH stretching and HNC and NCO bending at 3516.8, 3505.7 cm^{-1} and at 769.8 and 573.7 cm^{-1}, respectively. After deuterium substitution of the HNCO molecule, the NCO antisymmetric stretching, the ND stretching and the DNC and NCO bending vibrations appear at 2231.0, 2606.9 and at 578.6, 475.4 cm^{-1}, respectively.[33] In the studied spectra the most characteristic band within 1 band set is a broad absorption at *ca.* 2264 cm^{-1}, in the region of ν_{as}NCO. After deuterium substitution a narrow band at 2222.8 cm^{-1} appears in this region and is assigned to the perturbed NCO antisymmetric stretching vibration of DNCO. The broad band at *ca.* 2234 cm^{-1} is also observed in the vicinity of the ν_{as}NCO vibration of

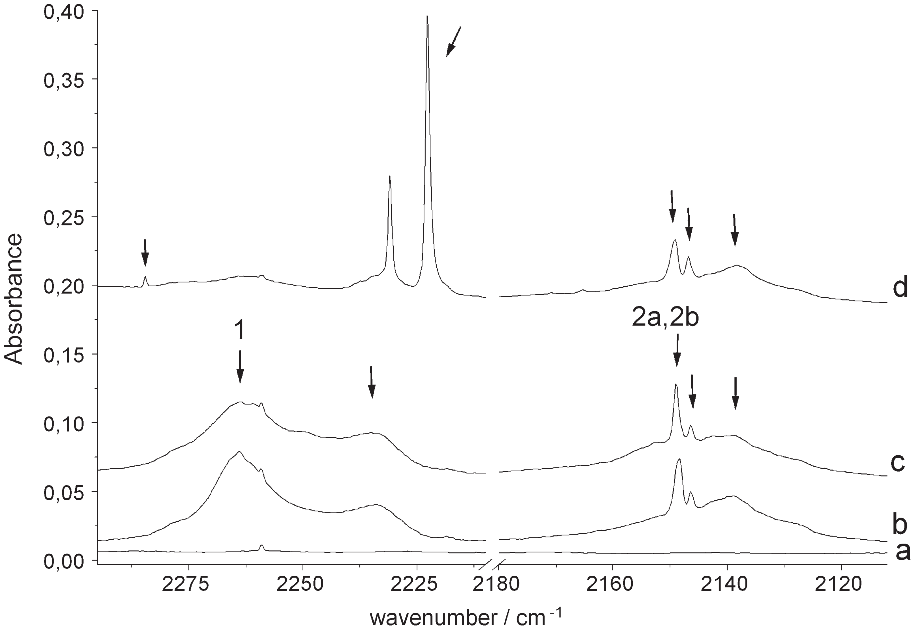

Fig. 2 The 2295–2110 cm^{-1} region in the spectra of the matrices (a, b, c) presented in Fig. 1. The spectrum of the $ND_2CONDOD/Ar$ matrix after matrix irradiation with the full output of the Xe arc lamp for 180 min (d) is also presented.

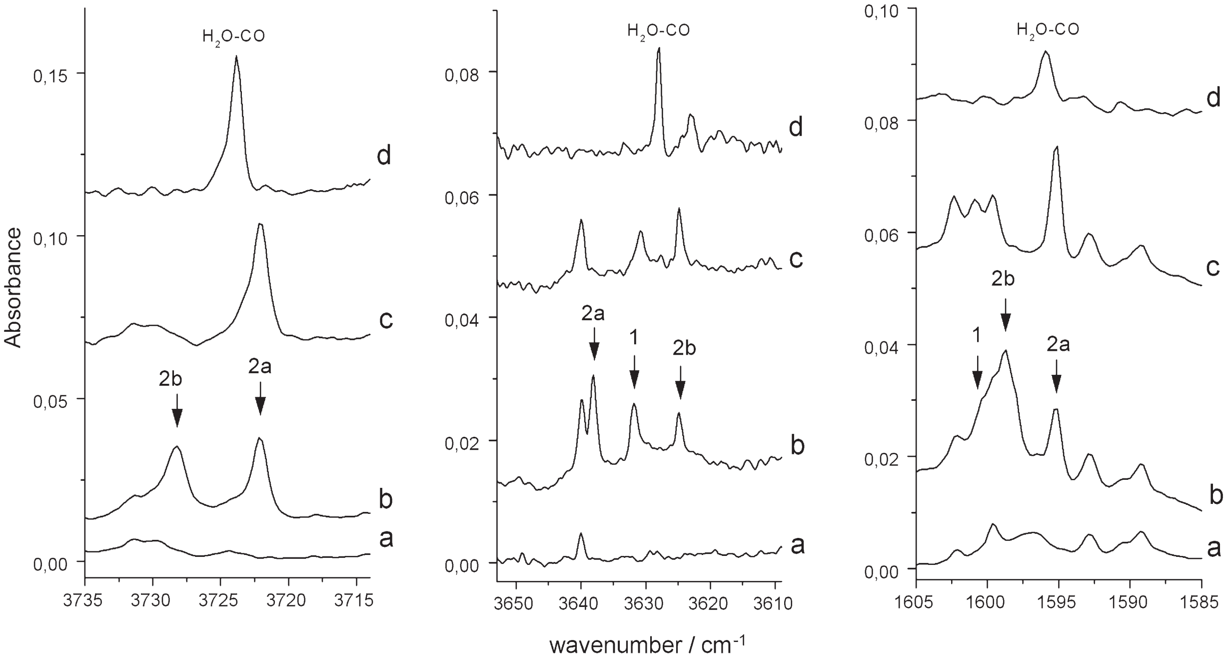

Fig. 3 The selected regions in the spectra of matrices (a, b, c) presented in Fig. 1. The spectrum of the H_2O/CO/Ar = 1 : 1 : 2000 matrix is also presented (d).

the HNCO monomer. The annealing experiments show the sensitivity of this band to the matrix temperature: the 2234 cm^{-1} band becomes more intense while the 2264 cm^{-1} one decreases upon the matrix annealing to 30 K for several minutes. This behaviour allows for the tentative assignment of the 2234 cm^{-1} band to the higher order HNCO–$(NH_2OH)_n$ complexes, it is most probably due to the HNCO–$(NH_2OH)_2$ complex. A similar pattern of absorptions in the region of the ν_{as}NCO vibration was reported for the HNCO–NH_3 system.[34] The broad band at *ca.* 2269 cm^{-1} was assigned to the HNCO–NH_3 complex, while the broad absorption at 2245 cm^{-1} was attributed to the HNCO–$(NH_3)_2$ complex.

The bands observed at 3287.9 and 3285.2 cm^{-1} are *ca.* 225 cm^{-1} shifted toward lower wavenumbers with respect to the

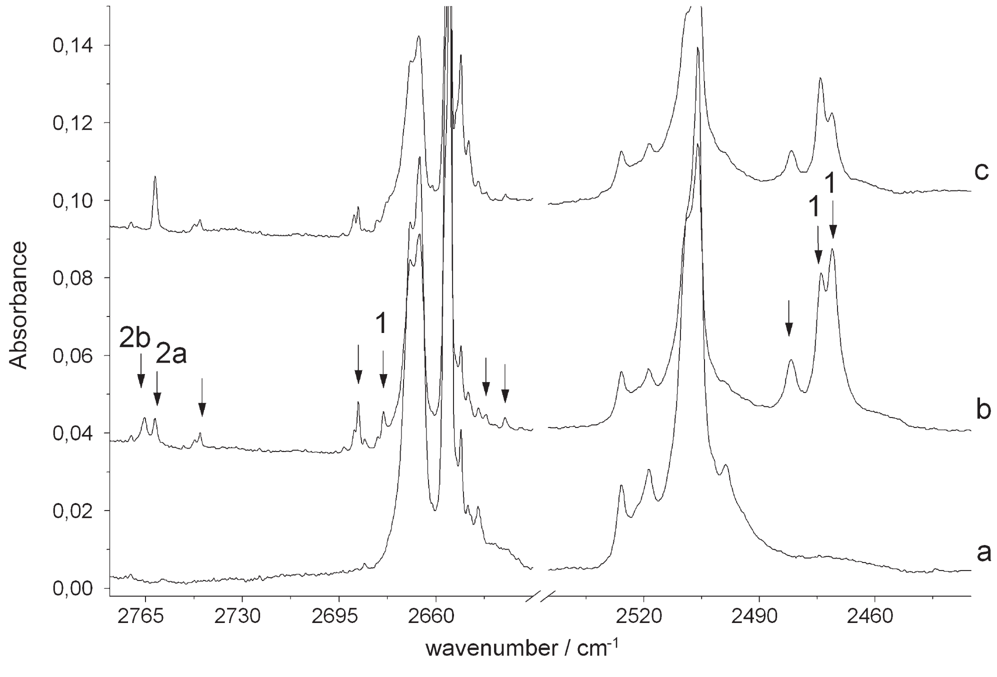

Fig. 4 The 2780–2435 cm^{-1} region in the spectra of matrices: $ND_2CONDOD$/Ar after matrix deposition at 15 K, spectrum measured at 9.5 K (a), after matrix irradiation with the full output of the Xe arc lamp for 180 min (b), and after annealing of matrix b for 10 min in 30 K, spectrum measured at 9.5 K (c).

Table 1 Observed absorptions (in cm^{-1}) after photolysis of *N*-hydroxyurea in solid argon

$NH_2CONHOH$	$ND_2CONDOD$	Species	Assignment
3728.4 (0.021)[a]	2765.5 (0.008)	N_2–H_2O–CO, N_2–D_2O–CO (2b)	$\nu_{as}H_2O$, $\nu_{as}D_2O$
3722.0 (0.018)	2761.5 (0.004)	N_2–H_2O–CO, N_2–D_2O–CO (2a)	$\nu_{as}H_2O$, $\nu_{as}D_2O$
3638.0 (0.015)		N_2–H_2O–CO (2b)	ν_sH_2O
	2747.5 (0.004)	D_2CO– D_2O	$\nu_{as}D_2O$
	2693.4 (0.001)	ND_2OD	νOD
	2689.5 (0.002)	ND_2OD	νOD
	2688.2 (0.008)	ND_2OD	νOD
3631.8 (0.006)	2681.0 (0.001)	HNCO–NH_2OH, DNCO–ND_2OD (1)	νOH, νOD
3630.6 (0.003)	2679.0 (0.004)	HNCO–NH_2OH, DNCO–ND_2OD (1)	νOH, νOD
3624.8 (0.004)		N_2–H_2O–CO (2a)	ν_sH_2O
	2642.0 (0.001)	D_2CO–HDO	ν_sHDO
	2635.0 (0.002)	DOCN	νOD
	2623.2 (0.001)	D_2CO–D_2O	ν_sD_2O
3295.2 (0.024)	2481.7 (0.014)	HNCO–H_2O, DNCO–D_2O	νNH, νND
3287.9 (0.062)	2473.8 (0.045)	HNCO–NH_2OH, DNCO–ND_2OD (1)	νNH, νND
3285.2 (0.06)	2471.0 (0.057)	HNCO–NH_2OH, DNCO–ND_2OD (1)	νNH, νND
2885.3 (0.001)		H_2CO–H_2O	$\nu_{as}CH_2$
2816.5 (0.003)	2084.7 (0.003)	H_2CO–H_2O, D_2CO–D_2O	ν_sCH_2 , ν_sCD_2
2796.0 (0.002)	2071.3	H_2CO, D_2CO	ν_sCH_2, ν_sCD_2
	2284.5 (0.002)	DOCN	νCN
	2235 br (0.011)	DNCO–D_2O	ν_{as}NCO
2264 br (0.65)	2222.8 (0.13)	HNCO–NH_2OH, DNCO–ND_2OD (1)	ν_{as}NCO
2234 br (0.3)		$(HNCO–NH_2OH)_n$	ν_{as}NCO
	2165.0 (0.002)	CO + ?	νCO
2148.9 (0.048)	2149.8 (0.05)	N_2–H_2O–CO, N_2–D_2O–CO (2a)	νCO
2148.5 (0.026)	2148.9 (0.03)	N_2–H_2O–CO, N_2–D_2O–CO (2b)	νCO
2146.3 (0.012)	2146.8 (0.022)	NH_2OH–CO, ND_2OD–CO	νCO
2142.6	2143.7	CO–NH, CO–ND	νCO
2138.4 br (0.16)	2138.4 br (0.11)	CO	νCO
	1690.9 (0.035)	D_2CO–H_2O	νC=O
1613.4 (0.001)	1184.2	HNCO–NH_2OH, DNCO–ND_2OD (1)	δNH_2, δND_2
1610.2 (0.001)	1190.0 (0.008)	H_2CO–H_2O, D_2CO–D_2O	δH_2O, δD_2O
1600.8 (0.004)	1174.0	NH_2OH–CO, ND_2OD–CO	δNH_2, δND_2
1598.7 (0.012)	1179.3 (0.01)	N_2–H_2O–CO, N_2–D_2O–CO (2b)	δH_2O, δD_2O
1595.0 (0.006)	1178.0 (0.01)	N_2–H_2O–CO, N_2–D_2O–CO (2a)	δH_2O, δD_2O
	1171.8 (0.003)	ND_2OD	δND_2
1499.0 (0.004)		H_2CO–H_2O	δCH_2
1173.8 (0.001)		H_2CO–H_2O	ωCH_2
	1077.6 (0.001)	DOCN	νC–O
1148.3 (0.014)	931.5 (0.005)	HNCO–NH_2OH, DNCO–ND_2OD (1)	ωNH_2, ωND_2
1121.6 (0.058)	922.8 (0.014)	NH_2OH–CO, ND_2OD–CO	ωNH_2, ωND_2
898.0 (0.002)		HNCO–NH_2OH (1)	δHNC
	816.5 (0.004)	DNCO–ND_2OD (1)	νNO
	850.0 (0.002)	?	
574.5 (0.003)		HNCO–H_2O	δNCO

[a] Integrated intensities are given in parentheses.

NH stretch of the HNCO monomer, such a large shift can be expected for HNCO serving as a proton donor in a hydrogen bonded complex. The ND stretch in the complex is identified at 2473.8 and 2471.0 cm^{-1}, showing a 134 cm^{-1} red shift with respect to νND in the DNCO molecule. A large perturbation of the NH stretch in the complex is probably responsible for the discrepancy between the deuterium shift of this vibration in free and complexed HNCO (904 and 814 cm^{-1}, respectively). The 898.0 cm^{-1} band is 128 cm^{-1} shifted toward higher wavenumbers, as compared to the unperturbed HNC bending vibration of the HNCO molecule. The position of this band suggests that the 898.0 cm^{-1} absorption corresponds to the perturbed HNC bending vibration of the bonded HNCO molecule. Unfortunately, no band corresponding to the perturbed DNC bending vibration of the complexed DNCO was identified.

The additional bands belonging to group 1 were found in the regions of the hydroxylamine molecule vibrations. The IR spectra of NH_2OH isolated in argon and nitrogen matrices are well known.[32,35] In the studied spectra, the 3631.8 and 3630.6 cm^{-1} bands are placed in the vicinity of the OH stretching vibration of the NH_2OH monomer (3634.7 cm^{-1}).[32] These bands appear at 2681.0 and 2679.0 cm^{-1} after deuterium substitution, showing the same −951 cm^{-1} deuterium shift within experimental error, as observed in the NH_2OH molecule (H/D = 1.35). The 1613.4 cm^{-1} band appears in the region of the NH_2 bending vibration of NH_2OH (1598.9 cm^{-1}) and shows a very similar deuterium shift to δNH_2 in the monomer (−429 cm^{-1} shift is observed for the 1613.4 cm^{-1} band and −428 cm^{-1} is reported for the 1598.9 cm^{-1} absorption).[32] The 1148.3 cm^{-1} band is observed in the vicinity of the NH_2 wagging vibration of the NH_2OH molecule (1117.0 cm^{-1}). The

1148.3 cm^{-1} band exhibits a similar deuterium shift (−216.8 cm^{-1}) to the ωNH_2 mode of the NH_2OH monomer (−202 cm^{-1}). The 816.5 cm^{-1} absorption is identified in the region of the νNO vibration of the ND_2OD molecule. Unfortunately no band corresponding to the perturbed NO stretch of NH_2OH was observed in the studied spectra.

The *ab initio* calculations demonstrate the stability of five hydrogen bonded structures of the HNCO–NH_2OH complex in which the OH or NH_2 group of hydroxylamine interacts with the NH group or the oxygen atom of the HNCO molecule. In Fig. S1,† all optimized structures of the HNCO–NH_2OH system are shown. The selected bond distances (in Å) and interaction energies (in kJ mol^{-1}) are also presented. The optimized geometrical parameters of the structures and the full set of vibrational wavenumbers are collected in Tables S1 and S2 (ESI †). Comparison of the experimental spectra with the calculated ones shows that the complex trapped in the matrix has the structure presented in Fig. 5, with the HNCO molecule acting as a proton donor toward the oxygen atom of hydroxylamine. There is an additional interaction between the NH_2 group of NH_2OH and the nitrogen atom of HNCO. It is worth mentioning that this structure is the second one in the calculated order of stability of five optimized complexes: it is 5.42 kJ mol^{-1} less stable than the most stable structure stabilized by the OH···N and NH···N hydrogen bonds.

The formation of the NH···O bond between the NH group of isocyanic acid and the oxygen atom of hydroxylamine is reflected in the calculated spectra by strong perturbations of the NH stretching and HNC bending vibrations of the HNCO and OH out of plane bending mode of NH_2OH. Table 2 presents the wavenumbers identified for the HNCO–NH_2OH and DNCO–ND_2OD complexes in an argon matrix and compares them with the calculated ones for the structure shown in Fig. 5. The appearance of the NH stretch at 3287.9, 3285.2 cm^{-1} provides very strong evidence for the formation of the HNCO–NH_2OH complex with a NH···O hydrogen bond. The observed red shift of these bands with respect to the HNCO monomer absorption (*ca.* −225 cm^{-1}) is in good agreement with the calculated shift value for this complex (−266 cm^{-1}). The deuterium counterparts of these bands show a *ca.* 134 cm^{-1} red shift with respect to the corresponding DNCO monomer vibration, which is in agreement with the calculated wavenumber shift (−186 cm^{-1}). The broad absorption at *ca.* 2264 cm^{-1}, assigned to the NCO antisymmetric stretching vibration, is 5 cm^{-1} shifted toward higher wavenumbers with respect to the monomer band, which is close to the predicted 3 cm^{-1} blue shift value. The 2264 cm^{-1} band shows the 8.2 cm^{-1} red shift on deuteration, which is in agreement with theoretical predictions (−13 cm^{-1}). The lower wavenumber of ν_{as}NCO in DNCO–ND_2OD than in HNCO–NH_2OH could be due to a 25% contribution of the ND stretching coordinate to the 2222.8 cm^{-1} vibration (Table 2). The band observed at 898.0 cm^{-1} is 128 cm^{-1} blue shifted, as compared to the unperturbed HNC bending vibration of the HNCO molecule, and this is in a good agreement with the calculated shift value (+93 cm^{-1}). The normal coordinate analysis indicates coupling between the δHNC, δNCO and γNCO internal coordinates. As a result, the NCO bending contributes to the 898.0 cm^{-1} normal mode, to which the largest contribution comes from δHNC. On deuteration, the γNCO internal coordinate gives an additional 38% contribution to the calculated 711 cm^{-1}, vibration and this probably causes a small 5 cm^{-1} red shift of the δDNC in the complex from the corresponding DNCO monomer absorption.

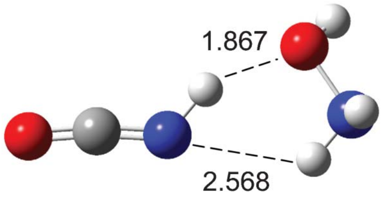

Fig. 5 The MP2/aug-cc-pVTZ optimized structure of the HNCO–NH_2OH complex (the selected bond distances (in Å); interaction energies $\Delta E^{CP} = -27.31$; $\Delta E^{CP}_{ZPE} = -21.23$ (in kJ mol^{-1})).

The identified hydroxylamine vibrations confirm the existence in matrices of the HNCO–NH_2OH complex of the structure shown in Fig. 5. The bands at 3631.8 and 3630.6 cm^{-1} are assigned to the stretching vibration of the OH group, which is only slightly perturbed after complex formation. The observed shift of these bands with respect to the OH stretch of the hydroxylamine monomer (*ca.* −4 cm^{-1}) is in good agreement with the predicted shift value (−9 cm^{-1}). The observed perturbations of the other hydroxylamine vibrations in both HNCO–NH_2OH and DNCO–ND_2OD complexes are also in good agreement with the calculated ones.

As one can see in Table S2,† all identified absorptions are predicted to be the most intense ones for the HNCO–NH_2OH complex with NH···O hydrogen bonding.

Formation of N_2–H_2O–CO complexes

The bands due to sets 2a and 2b appeared in the regions of the stretching and bending water vibrations[36] and in the vicinity of the CO monomer band.[29]

The 3728.4 (2b) and 3722.0 (2a) cm^{-1} absorptions are placed in the vicinity of the ν_{as} mode of the water molecule and show small 6.6 and 13 cm^{-1} red shifts from the H_2O monomer band. The deuterium counterparts of these bands are identified at 2765.5 (2b) and 2761.5 (2a) cm^{-1}, showing almost the same −963 and −961 cm^{-1} deuterium shifts as observed in the H_2O molecule (964 cm^{-1}). The 3638.0 (2b) and 3624.8 (2a) cm^{-1} bands appear in the vicinity of the ν_sH_2O vibration. Unfortunately their deuterium counterparts were not identified since they were expected in a complicated spectral region. The 1598.7 (2b) and 1595.0 (2a) cm^{-1} bands appearing in the vicinity of the bending mode of water are shifted 9.7 and 6 cm^{-1} toward higher wavenumbers, as compared to the unperturbed δH_2O vibration, and exhibit *ca.* −419 and −417 cm^{-1} deuterium shifts, respectively.

Additionally, the bands appearing in the region of the CO molecule vibration at 2148.9 (2a) and 2148.5 (2b) cm^{-1} (shifted to 2149.8 and 2148.9 cm^{-1} after deuteration, respectively) also show the behaviour of the bands of group 2a and 2b.

Decomposition of *N*-hydroxyurea leading to the formation of H_2O and CO, as indicated above, must also produce N_2 and H_2 species in the same matrix cage. Since the bands observed

Table 2 Wavenumbers and wavenumber shifts (in cm^{-1}), calculated and observed for the HNCO–NH$_2$OH complex in solid argon[a]

$NH_2O(H)\cdots HNCO$				$ND_2O(D)\cdots DNCO$				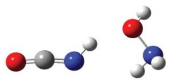
Experimental		Calculated		Experimental		Calculated		
ν	$\Delta\nu$	ν	$\Delta\nu$	ν	$\Delta\nu$	ν	$\Delta\nu$	Assignment[b,c]
3631.8	−4	3829	−9	2681.0	−5	2789	−8	νOH (100)
3630.6				2679.0				{νOD (100)}
3287.9	−225	3436	−266	2474.0	−134	2546	−186	νNH (100)
3285.2				2471.0				{νND (100)}
2264	+5	2321	+3	2222.8	−8.2	2280	−13	ν_{as}NCO (100)
								{ν_{as}NCO (75), νND (25)}
1613.4	+14.4	1673	+9	1184.2	+13.2	1212	+6	δNH_2 (88)
								{δND_2 (87)}
1148.3	+31.3	1166	+14	931.5	+16.5	844	+9	ωNH_2 (66), δOH (26)
								{ωND_2 (71), νNO (18)}
898.0	+128	888	+93	—	—	711	−5	δHNC (51), δNCO (33)
								{δDNC (40), γNCO (38), δNCO (11)}
—	—	932	−3	816.5	−2	939	−6	νNO (73), ωNH_2 (19)
								{νNO (61), δOD (38)}

[a] In all calculations the MP2/aug-cc-pVTZ method was used. [b] A potential energy distribution (PED) of the normal modes is presented; only the PED elements larger than 15% are shown. [c] The assignment for the DNCO–ND$_2$OD complex is given in brackets.

after matrix photolysis are not located at wavenumbers reported in literature for H$_2$O–CO[29] and H$_2$O–N$_2$ complexes,[37] there is a high probability that the ternary N$_2$–H$_2$O–CO complexes are formed. The question arises if the H$_2$ molecule stays in the argon cage or even in the vicinity, or does it possess enough energy from the decomposition process to leave the matrix cage. According to previous calculations results, the interaction energy between H$_2$ and each molecule discussed does not exceed 2.4 kJ mol^{-1} (*ca.* 0.9 kJ mol^{-1} for $H_2\cdots N_2$,[38] *ca.* 1.11 kJ mol^{-1} for $H_2\cdots CO$,[39] *ca.* 2.41 kJ mol^{-1} for $H_2\cdots H_2O$[40]). This fact points to a spontaneous decomposition of the aforementioned H$_2$ complexes to the separate monomers in solid argon at the temperatures used. Thus, taking into considerations the N$_2$ + H$_2$O + CO + H$_2$ system, H$_2$ is not involved as its fourth part and the final product would be the ternary N$_2$–H$_2$O–CO complex.

The performed calculations demonstrate the stability of three structures of the N$_2$–H$_2$O–CO complex that are shown in Fig. 6. The selected bond distances (in Å) and interaction energies (in kJ mol^{-1}) are also presented. In Table S3,† the geometrical parameters for the three structures are collected and in Tables 3 and S4† the calculated harmonic and anharmonic wavenumbers are presented. The most stable structure A, stabilized by the O–H···C(O) bond and van der Waals interaction between the N$_2$ and H$_2$O molecules, is 1.21 kJ mol^{-1} more stable than structure B, in which water acts as a proton donor forming the O–H···C and O–H···N hydrogen bonds. Structure A is also 1.31 kJ mol^{-1} more stable than structure C, in which water serves as a proton donor toward the nitrogen molecule forming the O–H···N(N) bond and the van der Waals interaction between CO and H$_2$O is also present. The formation of the O–H···C(O) hydrogen bonds in structures A and B is reflected in a similar decrease of the calculated $\nu_{as}H_2O$ and ν_sH_2O wavenumbers ($\Delta\nu_{calc}$ = −25 *vs.* −26 and −31 *vs.* −21 cm^{-1}, respectively) and an increase of the δH_2O and νCO wavenumbers ($\Delta\nu_{calc}$ = +7 *vs.* +10 and +13 *vs.* +11 cm^{-1}, respectively). The presence of the O–H···N hydrogen bond in structure C causes much less perturbation of the subunit vibrations. The comparison of the calculated wavenumbers for the three structures with absorptions identified in solid argon indicates that A and B complex structures are present in the matrix and they correspond to the 2a and 2b band sets, respectively.

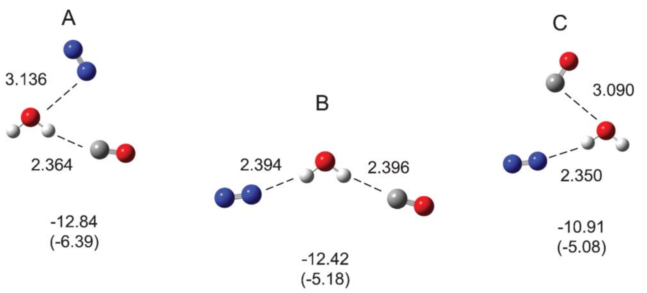

Fig. 6 The MP2/aug-cc-pVTZ optimized structures of the N$_2$–H$_2$O–CO complexes. The selected bond distances (in Å) and interaction energies ΔE^{CP} (in kJ mol^{-1}) are also presented; the $\Delta E^{CP}{}_{ZPE}$ values (in kJ mol^{-1}) are given in parentheses.

In relation to the experimental and theoretical data concerning the H$_2$O–CO system,[29,41–43] the calculations at the MP2/aug-cc-pVTZ level together with an argon matrix spectrum of the H$_2$O–CO complex were performed and the received results showed good agreement with the previous ones. Both the obtained theoretical wavenumber shifts with respect to the H$_2$O and CO monomers and the positions of the complex bands in solid argon demonstrate that the wavenumber values of H$_2$O–CO are located between those assigned to the N$_2$–H$_2$O–CO complex of structures A and B (see Table 3 and Fig. 3). The literature data show that water vibrations in a complex appear at 3723.5, 3627.8 and 1596.0 cm^{-1} for H$_2$O–CO and at 2762.7, 2650.1 and 1185.0 cm^{-1} for D$_2$O–CO and the

Table 3 Wavenumbers and wavenumber shifts (in cm^{-1}) calculated for the three structures of the N_2–H_2O–CO complexes and the corresponding values for the complexes observed in an argon matrix.[a] The calculated and observed values for the H_2O–CO complex are given for comparison

A				B				C			H_2O–CO				Assignment
$N_2\cdots(H)OH\cdots CO$				$N_2\cdots HOH\cdots CO$				$OC\cdots(H)OH\cdots N_2$							
ν harm	$\Delta\nu$	ν anh	$\Delta\nu$ obs	ν harm	$\Delta\nu$	ν anh	$\Delta\nu$ obs	ν harm	$\Delta\nu$	ν anh	ν harm	$\Delta\nu$	ν anh	$\Delta\nu$ obs[b]	
3926	−25	3749	−13.0	3925	−26	3756	−6.6	3935	−16	3757	3932	−19	3755	−11.5	$\nu_{as}H_2O$
3794	−31	3632	−13.7	3804	−21	3648	−0.5	3810	−15	3645	3802	−23	3644	−10.2	ν_sH_2O
1636	+8	1585	+5	1638	+10	1580	+8.7	1632	+4	1584	1635	+7	1584	+7	δH_2O
2123	+13	2093	+10.4	2121	+11	2090	+10	2115	+5	2089	2123	+13	2098	+11	νCO
2186	+1	2146	—	2189	+2	2151	—	2189	+2	2150	—	—	—		νN_2

[a] In all calculations the MP2/aug-cc-pVTZ method was used. [b] See ref. 29.

CO molecule perturbations are observed at 2149.4 cm^{-1} and 2150.2 cm^{-1} for both these systems,[29,41] respectively.

Photodissociation of HU - formation of the HNCO–NH_2OH and N_2–H_2O–CO complexes

Analysis of the spectra of the $NH_2CONHOH$/Ar matrices irradiated with Xe arc lamp output proves the existence of two photodissociation channels of $NH_2CONHOH$ under the conditions of this experiment:

$$NH_2CONHOH \rightarrow HNCO + NH_2OH \quad (1)$$

$$\begin{aligned} NH_2CONHOH &\rightarrow (NH_2NHOH + CO \rightarrow N_2H_2 + H_2O + CO) \\ &\rightarrow H_2 + N_2 + H_2O + CO \end{aligned} \quad (2)$$

The products of each photodissociation reaction are trapped in the original precursor site in the matrix, resulting in the formation of the HNCO–NH_2OH and N_2–H_2O–CO complexes. However, very weak absorptions due to the NH_2OH, HNCO, HOCN and CO monomers are also detectable. A cage exit probability of small photo fragments is enhanced by an excess of energy, which they have after decomposition of the precursor, and depends on the interactive forces between the fragment and the surrounding cage. The photon absorption may induce even long-range migration of fluorine, oxygen and hydrogen atoms, moving them several lattice sites away from their origin. The barrier for the cage exit of the hydrogen atom in rare gas solids is 1–1.5 eV (96–145 kJ mol^{-1}), which stays within the range of the studied experiment.[44,45] The NCO radicals were not observed during photolysis of HNCO in an Ar matrix with a medium pressure mercury lamp. However the radicals were formed when the matrix was irradiated with VUV radiation at 121.6 nm.[30] This could be explained by the cage exit of the hydrogen atom with a larger excess of energy. The photodissociation of ozone in solid argon at 266 nm resulted in recombination of O + O_2 as a major pathway and the decrease of ozone was due to a cage exit of oxygen atoms, which depended on the temperature and irradiation power.[46] The cage exit probability for an OH radical in 230 nm photolysis of H_2O_2 was found to be 17% in Ar at 17 K.[47]

The photochemical studies of formohydroxamic acid[24] and formamide[48] show that the $n \rightarrow \pi^*$ excitation within the carbonyl moiety in simple amide molecules leads to the excited singlet state in which cleavage of the C–N bond occurs (α-cleavage), and in the case of substituted hydroxamic acids a scission of the N–O bond also takes place. Recently, the mechanistic photochemistry of urea was studied by means of *ab initio* calculations on the stationary and intersection structures in the lowest three energy states,[49] which gave new insight into the mechanism proposed experimentally in low temperature matrices upon VUV irradiation at wavelengths of $\lambda > 160$ nm.[50] Based on these studies, the formation of the HNCO–NH_2OH and N_2–H_2O–CO complexes, as the major photoproducts of HU, can be proposed. Scheme 1 gives the mechanistic view, indicating the routes toward new species. The deamination reaction ($NH_2CONHOH \rightarrow HNCO + NH_2OH$) may occur in the S_0 state after a very fast $S_1 \rightarrow S_0$ internal conversion (like in the case of the urea molecule). It is a single step reaction in which one hydrogen atom of the NH_2 group transfers to the nitrogen atom of the NHOH group and then the C–N bond dissociates, forming HNCO and NH_2OH and finally the HNCO–NH_2OH complex. The next possibility of deamination is at first a scission of the N–O bond and production of $NH_2C(O)NH$ + OH radicals. Then, the hot $NH_2C(O)NH$ radical disintegrates into NH_2 + C(O)NH, and the HNCO + NH_2OH products are formed. The other channel for the NH_2OH formation is a two step reaction in which at first an isomerization reaction $NH_2CONHOH \rightarrow NH_2(HO)C{=}NOH$ occurs, and then the OH radical is created and transferred to the NH_2 group and NH_2OH forms. However, the last mechanism seems unlikely, since the iminol tautomers of HU are substantially less stable than the keto forms (40–85 kJ mol^{-1})[51] and have not been identified experimentally so far. Isourea, $NH_2(HO)C{=}NH$, was observed upon VUV irradiation of urea in argon and xenon matrices as an intermediate product converted in a dehydration reaction to the NH_2CN–H_2O complex.[50] The excited S_1 state can decay to the T_1 state *via* the $S_1 \rightarrow T_1$ intersystem crossing and then the C–N bond fission would create the NH_2CO and NHOH radicals. The hot NH_2CO radical dissociates into NH_2 + CO and then the NH_2 and NHOH radicals could recombine forming *N*-hydroxyhydrazine, NH_2NHOH. This very unstable molecule was observed experimentally by Andrews *et al.*[52] as the product of the reaction between hydrazine and ozone during deposition in an argon matrix. Despite a very careful analysis of the observed spectra, no bands expected in the regions of *N*-hydroxyhydrazine vibrations were identified. This indicates that the fast decomposition process proceeds: $NH_2NHOH \rightarrow$

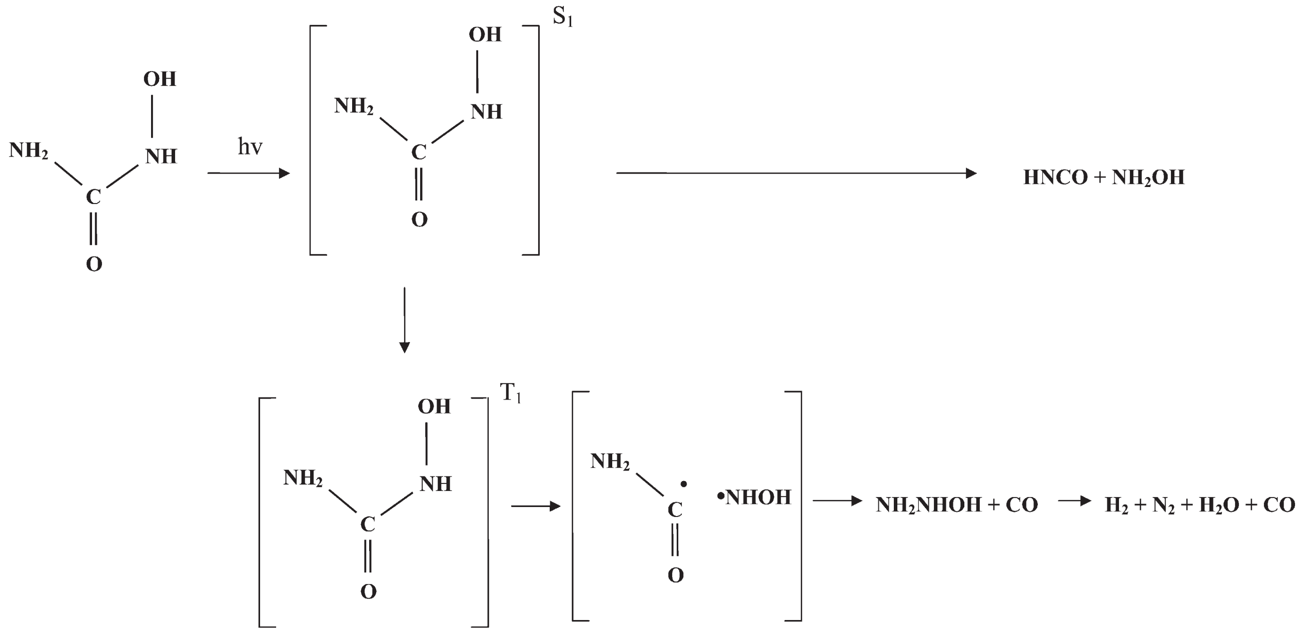

Scheme 1 Possible mechanism of the formation of $HNCO + NH_2OH$ and $H_2 + N_2 + H_2O + CO$ photoproducts from *N*-hydroxyurea.

$(N_2H_2 + H_2O) \rightarrow N_2 + H_2 + H_2O$, and finally the N_2, H_2O and CO molecules trapped in the same cage form the N_2–H_2O–CO complexes (migration of hydrogen atoms in an argon matrix was already discussed). The matrix isolated diazene molecule, N_2H_2, was recognized to be one of the secondary products during photolysis of urea[50] or the NH_3–CO_2 complex,[53] but there are no absorptions that could be assigned to the N_2H_2 vibrations in the studied spectra.

The performed study does not allow us to draw any definitive conclusions concerning the electronic states that lead to the observed reaction channels, as the matrices were irradiated with the broad band irradiation of the Xe arc lamp, and the excited electronic states of the HU molecule have not, to my knowledge, been studied so far. The similarity of the products formed during photolysis of *N*-hydroxyurea and urea suggests comparable mechanisms of photodecomposition of these molecules. The photodissociation process of *N*-hydroxyurea gives $HNCO + NH_2OH$ and $H_2 + N_2 + H_2O + CO$ products under the conditions of the experiment and photodecomposition of urea (NH_2CONH_2) leads mainly to $HNCO + NH_3$ and $N_2H_4 + CO$ products. If a similar mechanism of photodissociation for these molecules is assumed and the results of the high level calculations of photochemical pathways of urea are taken into consideration,[49] then it follows that the deamination reaction proceeds at the S_0 state after fast $S_1 \rightarrow S_0$ internal conversion and the C–N bond cleavage occurs in the T_1 state as a result of the $S_1 \rightarrow T_1$ intersystem crossing. However, this is still a possible mechanism of photodecomposition of HU and, based on the experimental results, *ab initio* calculations of the ground and excited states are necessary to improve the reaction pathways. There are two factors that might have a significant influence on the obtained results. First, the presence of the oxygen atom of the OH group in the HU molecule changes the electron density distribution on nitrogen and carbon atoms as compared to urea, and affects the excited states of the molecule. Second, the broad band excitation of the HU molecule may also affect the efficiency of the intersystem crossing to a triplet state.

Other photolysis products

The very weak absorptions due to the CO, hydroxylamine (ND_2OD) and cyanic acid (DOCN) monomers that appeared in the spectra of irradiated matrices indicate that under the conditions of the experiment a small number of these molecules can escape from the parent cage. The escaping molecules can form molecular complexes with other molecules present in the matrix. The weak bands at 3295.2, 574.5 cm^{-1} and 2146.3, 1600.8 and 1121.6 cm^{-1} are attributed to the $HNCO$–H_2O and NH_2OH–CO complexes, respectively.[24]

The very weak absorptions at 2635.0, 2284.5, 1077.6 cm^{-1} are due to the DOCN molecule,[33] and the band at 2142.6 (2143.7) cm^{-1} is assigned to the NH–CO (ND–CO) complex.[30] These species most probably originate from the HNCO molecule formed on irradiation and having undergone further reactions. The literature reports on the photoequilibrium between HNCO and HOCN observed during irradiation with $\lambda > 224$ nm of the HNCO molecule isolated in solid argon.[54] The photodecomposition of HNCO and formation of the NH–CO complexes were also observed.[30]

On the basis of the literature data,[31] the very weak absorptions at 2885.3, 2816.5, 1610.2, 1499.0 and 1173.8 cm^{-1} are assigned to the H_2CO–H_2O complex and the 2796.0 cm^{-1} band is due to the H_2CO monomer. The formation of H_2CO and H_2CO–H_2O during UV-Vis irradiation of HU needs some comment. Formaldehyde was not identified as a photodissociation product of simple hydroxamic acids, but the molecule was formed in photodecomposition reactions of urea, as the secondary species originated from the primary

CO–N_2H_4 complex.[50] It was suggested that H_2CO + N_2H_2 products arise from the radical pair HCO + N_2H_3 produced during excitation of the CO–N_2H_4 complex; the formation of the HCO radical was also confirmed. In the case of HU photolysis, a much more possible mechanism leading to the H_2CO formation seems to be the hydrogenation of CO. The C–N bond cleavage of the *N*-hydroxyurea molecule creates the NH_2CO and NHOH radicals that undergo further photochemical reactions, resulting in CO and most probably NH_2NHOH (as discussed above). Hydrogen atoms formed in a decomposition process of NH_2NHOH (together with the identified N_2 and H_2O molecules) react with CO molecules present in the same matrix cage, and finally H_2CO is produced. In this manner, the formation of H_2CO becomes indirect proof of hydrogen migration in the studied argon matrices. Recently, the successive hydrogenation of CO was studied by co-injection of CO molecules and H atoms at 3 and 10 K.[55] The obtained results showed that in the CO + H reaction, H_2CO and CH_3OH, together with HCO and CH_3O species were formed.

4. Conclusions

The irradiation of *N*-hydroxyurea isolated in an argon matrix with the full output of the Xe arc lamp leads to HNCO + NH_2OH and H_2 + N_2 + H_2O + CO product species, which suggests two photodissociation pathways. The deamination reaction, resulting in hydroxylamine formation, can proceed at the S_0 state after fast $S_1 \rightarrow S_0$ internal conversion, whereas the C–N bond cleavage, in which the radicals are formed, can occur in the T_1 state as a result of $S_1 \rightarrow T_1$ intersystem crossing. The photolysis products trapped in the same cage form $NH_2O(H)\cdots HNCO$, $N_2\cdots(H)OH\cdots CO$ and $N_2\cdots HOH\cdots CO$ complexes. The calculations at the MP2/aug-cc-pVTZ level demonstrate the stability of five structures for the isocyanic acid–hydroxylamine complex and three structures for the nitrogen–water–carbon monoxide complex. The calculations predict the $NH_2O(H)\cdots HNCO$ complex with HNCO hydrogen bonded to the oxygen atom of the hydroxylamine molecule to be 5.42 kJ mol^{-1} less stable than the most stable structure in which the OH⋯N and NH⋯N hydrogen bonds are present. In turn, the most stable $N_2\cdots(H)OH\cdots CO$ complex stabilized by the O–H⋯C(O) hydrogen bond and van der Waals interaction between the N_2 and H_2O molecules is calculated to be 1.21 kJ mol^{-1} more stable than the $N_2\cdots HOH\cdots CO$ complex, with water acting as a proton donor toward the nitrogen and carbon atoms of N_2 and CO molecules, respectively.

Since *N*-hydroxyurea demonstrates a wide spectrum of biomedical therapeutic applications, acting mainly as a nitric oxide and nitric oxide-related donor, it was interesting to see the influence of UV-Vis irradiation on the NO (or HNO) formation mechanism from the isolated HU molecule. In a recent review,[56] *N*-hydroxyurea was reported to release nitric oxide (or nitroxyl) *via* oxidation reactions, proceeding through the nitroxide radical or *C*-nitrosoformamide as intermediates. A careful spectral analysis excluded formation of these products from a photodecomposition process of HU, in agreement with the proposed photochemical pathways. Neither the deamination reaction nor the C–N bond cleavage lead to nitroxide radical or *C*-nitrosoformamide. The performed experimental studies clearly show the absence of a photodissociation channel, converting the isolated *N*-hydroxyurea molecule to NO or HNO species.

Acknowledgements

The author gratefully acknowledges a grant of computer time from the Wrocław Center for Networking and Supercomputing.

References

1 W. F. C. Dresler and R. Stein, *Justus Liebigs Ann. Chem.*, 1869, **150**, 242.

2 J. W. Yarbro, B. J. Kennedy and C. P. Barnum, *Proc. Natl. Acad. Sci. U. S. A.*, 1965, **53**, 1033.

3 I. H. Krakoff, N. C. Brown and P. Reichard, *Cancer. Res.*, 1968, **28**, 1559.

4 S. Nyholm, L. Thelander and A. Graeslund, *Biochemistry*, 1993, **32**, 11569.

5 A. S. Boyd and K. H. Neldner, *J. Am. Acad. Dermatol.*, 1991, **25**, 518.

6 A. M. Layton, R. A. Sheehan-Dare, M. J. D. Goodfield and J. A. Cotterill, *Br. J. Dermatol.*, 1989, **121**, 647.

7 M. Piver, M. Khalil and L. J. Emrich, *J. Surg. Oncol.*, 1989, **42**, 120.

8 M. H. Steinberg, F. Barton, O. Castro, C. H. Pegelow, S. K. Ballas, A. Kutlar, E. Orringer, R. Bellevue, N. Olivieri, J. Eckman, M. Varma, G. Ramirez, B. Adler, W. Smith, T. Carlos, K. Ataga, L. DeCastro, C. Bigelow, Y. Saunthararajah, M. Telfer, E. Vichinsky, S. Claster, S. Shurin, K. Bridges, M. Waclawiw, D. Bonds and M. Terrin, *JAMA, J. Am. Med. Assoc.*, 2003, **289**, 1645.

9 F. Lori, A. Malykh, A. Cara, D. Sun, J. N. Weinstein, J. Lisziewicz and R. C. Gallo, *Science*, 1994, **266**, 801.

10 M. A. Gibbs and S. J. Sorensen, *Ann. Pharmacother.*, 2000, **34**, 89.

11 S. B. King, *Free Radical Biol. Med.*, 2004, **37**, 737.

12 M. T. Gladwin and A. N. Schechter, *Semin. Hematol.*, 2001, **38**, 333.

13 J. Huang, E. Sommers, D. B. Kim-Shapiro and S. B. King, *J. Am. Chem. Soc.*, 2002, **124**, 3473.

14 C. Walling and A. N. Naglieri, *J. Am. Chem. Soc.*, 1960, **82**, 1820.

15 E. Lipczynska-Kochany and J. Kochany, *J. Photochem. Photobiol., A*, 1988, **44**, 317.

16 E. Lipczynska-Kochany, H. Iwamura and J. Kochany, *Monatsh. Chem.*, 1987, **118**, 1345.

17 E. Lipczynska-Kochany and J. Kochany, *J. Photochem.*, 1987, **38**, 331.

18 P. N. Chhaya, M. M. Nimbalkar and B. D. Hosangadi, *Tetrahedron Lett.*, 1983, **24**, 5551.

19 B. D. Hosangadi, P. N. Chhaya, M.M. Nimbalkar and N. R. Patel, *Tetrahedron*, 1987, **43**, 5375.

20 D. Hosangadi, M. M. Nimbalkar and N. R. Patel, *Tetrahedron*, 1988, **44**, 5857.
21 J. E. Johnson, M. Arfan, R. Hodzi, L. R. Caswell and S. Rasmussen, *Photochem. Photobiol.*, 1990, **51**, 139.
22 E. Lipczyńska-Kochany, *Chem. Rev.*, 1991, **91**, 477.
23 M. Sałdyka, *Phys. Chem. Chem. Phys.*, 2010, **12**, 15111.
24 M. Sałdyka and Z. Mielke, *Phys. Chem. Chem. Phys.*, 2003, **5**, 4790.
25 M. J. Frisch, G. W. Trucks, H. B. Schlegel, G.E. Scuseria, M. A. Robb, J. R. Cheeseman, G. Scalmani, V. Barone, B. Mennucci, G. A. Petersson, H. Nakatsuji, M. Caricato, X. Li, H.P. Hratchian, A. F. Izmaylov, J. Bloino, G. Zheng, J. L. Sonnenberg, M. Hada, M. Ehara, K. Toyota, R. Fukuda, J. Hasegawa, M. Ishida, T. Nakajima, Y. Honda, O. Kitao, H. Nakai, T. Vreven, J. A. Montgomery Jr., J. E. Peralta, F. Ogliaro, M. Bearpark, J. J. Heyd, E. Brothers, K. N. Kudin, V. N. Staroverov, T. Keith, R. Kobayashi, J. Normand, K. Raghavachari, A. Rendell, J. C. Burant, S. S. Iyengar, J. Tomasi, M. Cossi, N. Rega, J. M. Millam, M. Klene, J. E. Knox, J. B. Cross, V. Bakken, C. Adamo, J. Jaramillo, R. Gomperts, R. E. Stratmann, O. Yazyev, A. J. Austin, R. Cammi, C. Pomelli, J. W. Ochterski, R. L. Martin, K. Morokuma, V. G. Zakrzewski, G. A. Voth, P. Salvador, J. J. Dannenberg, S. Dapprich, A. D. Daniels, O. Farkas, J. B. Foresman, J. V.Ortiz and J. Cioslowskiand D. J. Fox, *GAUSSIAN 09 (Revision B.01)*, Gaussian, Inc., Wallingford CT, 2010.
26 S. F. Boys and F. Bernardi, *Mol. Phys.*, 1970, **19**, 553.
27 J. S. Simon, M. Duran and J. J. Dannenberg, *J. Chem. Phys.*, 1996, **105**, 11024.
28 J. M. L. Martin and C. Van Alsenoy, *GAR2PED*, University of Antwerp, Antwerpen, Belgium, 1995.
29 H. Abe and K. M. T. Yamada, *J. Chem. Phys.*, 2001, **114**, 6134.
30 D. E. Milligan and M. E. Jacox, *J. Chem. Phys.*, 1967, **47**, 5157.
31 B. Nelander, *Chem. Phys.*, 1992, **159**, 281.
32 R. Withnall and L. Andrews, *J. Phys. Chem.*, 1988, **92**, 2155.
33 J. H. Teles, G. Maier, B. A. Hess Jr., L. J. Schaad, M. Winnewisser and B. P. Winnewiser, *Chem. Ber.*, 1989, **122**, 753.
34 S. Raunier, T. Chiavassa, F. Marinelli, A. Allouche and J.-P. Aycard, *J. Phys. Chem. A*, 2003, **107**, 9335.
35 G. A. Yeo and T. A. Ford, *J. Mol. Struct.*, 1990, **217**, 307.
36 A. Engdahl and B. Nelander, *J. Mol. Struct.*, 1989, **193**, 101.
37 S. Coussan, A. Loutellier, J. P. Perchard, S. Racine and Y. Bouteiller, *J. Mol. Struct.*, 1998, **471**, 37.
38 P. Hobza and R. Zahradník, *Chem. Rev.*, 1988, **88**, 871.
39 P. Jankowski and K. Szalewicz, *J. Chem. Phys.*, 2005, **123**, 104301.
40 J. Sadlej, B. Rowland, J. P. Devlin and V. Buch, *J. Chem. Phys.*, 1995, **102**, 4804.
41 T. Svensson and B. Nelander, *Chem. Phys.*, 2000, **262**, 445.
42 J. Lundell, *J. Phys. Chem.*, 1995, **99**, 14290.
43 J. Langlet, J. Caillet and M. Allavena, *J. Mol. Struct.*, 1998, **450**, 69.
44 K. H. Godderz, N. Schwentner and M. Chergui, *J. Chem. Phys.*, 1996, **105**, 451.
45 V. A. Apkarian and N. Schwentner, *Chem. Rev.*, 1999, **99**, 1481.
46 M. Bahou, L. Schriver-Mazzuoli and A. Schriver, *J. Chem. Phys.*, 1999, **110**, 8636.
47 L. Khriachtchev, M. Pettersson, S. Tuominen and M. Räsänen, *J. Chem. Phys.*, 1997, **107**, 7252.
48 J. Lundell, M. Krajewska and M. Räsänen, *J. Phys. Chem. A*, 1998, **102**, 6643.
49 G. Cui, L. Ding, F. Feng, Y. Liu and W. Fang, *J. Chem. Phys.*, 2010, **132**, 194308.
50 F. Duvernay, T. Chiavassa, F. Borget and J.-P. Aycard, *J. Phys. Chem. A*, 2005, **109**, 6008.
51 M. Remko, P. D. Lyne and W. G. Richards, *Phys. Chem. Chem. Phys.*, 1991, **1**, 5353.
52 R. Lascola, R. Withnall and L. Andrews, *Inorg. Chem.*, 1988, **27**, 642.
53 J. B. Bossa, F. Duvernay, P. Theulé, F. Borget and T. Chiavassa, *Chem. Phys.*, 2008, **354**, 211.
54 M. E. Jacox and D. E. Milligan, *J. Chem. Phys.*, 1964, **40**, 2457.
55 C. Pirim, L. Krim, C. Laffon, Ph. Parent, F. Pauzat, J. Pilmé and Y. Ellinger, *J. Phys. Chem. A*, 2010, **114**, 3320.
56 S. B. King, *Curr. Top. Med. Chem.*, 2005, **5**, 665.